ORILAM, A three moment lognormal aerosol scheme for mesoscale atmospheric model. On-line coupling into the Meso-NH-C model and validation on the Escompte campaign.

Pierre Tulet, Vincent Crassier[1], Frederic Cousin[2] Karsten Suhre[3] and Robert Rosset[2]

CNRM/GMEI Météo France, 42 av G. Coriolis, 31057 Toulouse, France

Short title: ORILAM SCHEME

[1]ORAMIP, 19 Avenue Clément ADER 31770 Colomiers, France

[2]LA / OMP, 14 av Ed Belin, 31400 Toulouse France

[3]IGS, UPR CNRS 2589, 31, chemin Joseph Aiguier, 13402 Marseille Cedex 20, France

Abstract. Classical aerosol schemes use either a sectional (bin) or lognormal approach. Both approaches have particular capabilities and interests: the sectional approach is able to describe every kind of distribution whereas lognormal one makes assumption of the distribution form with a fewer number of explicit variables. For this last reason we developed a-three moment lognormal aerosol scheme named ORILAM to be coupled in three-dimensional mesoscale or CTM models. This paper presents the concept and hypothesis of a range of aerosol processes such as nucleation, coagulation, condensation, sedimentation, and dry deposition. One particular interest of ORILAM is to keep explicit the aerosol composition and distribution (mass of each constituent, mean radius and standard deviation of the distribution are explicit) using the prediction of three moments (m0, m3 and m6).

The new model was evaluated by comparing simulations to measurements from the Escompte campaign and to a previously published aerosol model. The numerical cost of the lognormal mode is lower than two bins of the sectional one.

1. Introduction

During the last twenty years, some simulations of tropospheric aerosols with a large level of complexity have appeared. Trajectory models have been used by *Russell and Cass* [1986] for nitric aerosols and by *Pandis et al.* [1993] for secondary organic aerosols. *Wexler et al.* [1994] described methods and a theoretical formalism relative to bin aerosol approach to be used in atmospheric eulerian models. This kind of models have been used for heterogeneous pollution studies with various numbers of bins and chemical species (i.e. [*Pilinis and Seinfeld*, 1987], [*Jacobson et al.*, 1996], [*Lurmann et al.*, 1997], [*Sun and Wexler*, 1998], [*Meng et al.*, 1998], [*Pai et al.*, 2000], [*Griffin et al.*, 2002], [*Zhang et al.*, 2004]). *Binkowski and Shankar* [1995] introduced the modal approach based on the *Whitby et al.* [1991] aerosol formulation in their regional eulerian model RPM on northeastern american coast. The development and the application of aerosol models in Europe appeared later. *Wilson* [1996] developed a modal aerosol model based on the bin model of *Raes et al.* [1992], and used it in a three-dimensional eulerian model. *Ackermann et al.* [1998] first introduced a three-dimensional approach with a log-normal model issued from the study by *Binkowski and Shankar* [1995].

This paper aims at presenting a new log-normal model, named ORILAM (ORganic Inorganic Log-normal Aerosol Model), with the specificity of an explicit third moment (section 3). On the assumption of a log-normal distribution, ORILAM predicts the evolution of this aerosol distribution in time and space. This approach permits an explicit evolution of the aerosol composition, the number, the mean radius and the standard deviation of the aerosol distribution [*Binkowski and Roselle*, 2003]. These parameters

are important if we consider the action and retro-action of aerosol on radiation and cloud condensation nuclei activation classically used in atmospheric models. The ORILAM aerosol scheme has been introduced on-line in the MesoNH-C mesoscale atmospheric model [*Lafore et al.*, 1998]; [*Suhre et al.*, 1998]; [*Mari et al.*, 2000] and [*Tulet et al.*, 2003]. A 1D preliminary version of ORILAM was used during three IOP of the ACE2 experiment [*Suhre et al.*, 2000]. The results proved the capability of the log-normal approach to simulate the evolution of marine aerosols.

The Escompte 2001 campaign [*Cros et al.*, 2004] with an exhaustive set of dynamical, radiative, gas and aerosol data is used as a first three- dimensional case study to evaluate ORILAM/Meso-NH-C capability. The new model is evaluated against measurements and a previous bin model study from the same campaign ([*Bessagnet and Rosset*, 2001]; [*Cousin et al.*, 2004]).

2. Aerosol size distribution: sectional and log-normal approaches

Most aerosol schemes use a sectional distribution approach dividing the size range of the particle size distribution into a set of size sections; [*Wexler et al.*, 1994]; [*Pilinis and Seinfeld*, 1987]; [*Jacobson*, 1997] [*Jacobson*, 1999]. This method is better to determine free size distribution but involves a significant number of variables to give a realistic aerosol spectrum. Another way is to consider a modal approach based on *Whitby et al.* [1991] formulation, and developed in the CMAQ model by *Binkowski and Shankar* [1995].

The aim of sectional approach is a continuum size distribution of a finite number of sections in which one moment of the spectral distribution is constant (classicaly the mass $dM_3/d(\log(r_p))$). These assumptions consequently introduce an aerosol distribution

with a histogram form. Most of sectional techniques clearly involve that the boundary between sections is fixed in time. This particularity introduces a numerical diffusion in particular when an initial large size distribution narrows by increasing the aerosol volume. Nevertheless, this numerical diffusion is reduced with the use of variable section diameters [*Jacobson*, 1999]. In addition, the precision of the sectional approach depends on the number of sections. In the modal approach the aerosol population is composed of a few number of modes that partially intersect. For example this is the aerosol spectral distribution choosen by *Whitby et al.* [1991]; *Binkowski and Shankar* [1995]; *Whitby and McMurry* [1997]; *Ackermann et al.* [1998]. The major limitation of this approach is that the number of modes needs to be preliminary fixed. Several studies give some comparisons between both approaches [*Seigneur et al.*, 1986]; [*Tsang and Rao*, 1988]; [*Harrington and Kreidenweis*, 1998], [*Zhang et al.*]: *Seigneur et al.* [1986] have compared coagulation - condensation processes for continuum, sectional and log-normal models. They found that the log-normal model reproduces every size distribution with an error smaller than 20% in comparison with the continuum model, and is 40 times faster than the sectional model. *Harrington and Kreidenweis* [1998] found same results whereas modal schemes give better results for an equal number of equations to solve. For numerical cost and precision we choose a log-normal aerosol formulation to be coupled in three-dimensionnal atmospheric model.

3. General description

The prognostic evolution of the aerosol size distribution is determined by a general dynamical equation [*Friedlander*, 1977]; [*Seinfeld and Pandis*, 1997] without analytical solution:

$$\frac{\partial n(r_p)}{\partial t} = f(n(r_p)) \tag{1}$$

where n is the function of aerosol size distribution ($particles/cm^3$) and r_p is the aerosol radius (μm). This equation can be integrated to obtain an equation system such as:

$$\frac{\partial M_k}{\partial t} = f(M_k) \tag{2}$$

where the k^{th} moment is given by $M_k = \int_0^\infty r_p^k n(r_p) dr_p$ ($\mu m^k/cm^3$). Using several assumptions (choice of the aerosol spectral distribution) the equation system 2 can be closed giving $f(M_k)$ in terms of moments. Three modes have been implemented; the first one to represent the new particles formed (nuclei mode); the second one for bigger and evoluted particles (accumulation mode); the last one is devoted to dust particles and introduced as a passive mode (no interaction with the nuclei and accumulation mode). Each mode is represented by a log-normal distribution as:

$$n(\ln D) = \frac{N}{\sqrt{2\pi}\ln\sigma_g} \exp\left(-\frac{\ln^2(\frac{D}{D_g})}{2\ln^2(\sigma_g)}\right) \tag{3}$$

where N is the particle number concentration (in $particles/cm^3$), D is the particle diameter (μm) and D_g , σ_g are respectively the number median diameter and the geometric standard deviation of the modal distribution. The k^{th} moment of the mode i is defined as :

$$M_{k,i} = \int_0^\infty r^k n_i(r) dr \tag{4}$$

After integration (variable change as $x = \frac{\ln(r/D_g)}{\ln(\sigma)}$) we obtain:

$$M_{k,i} = N R_g^k \exp\left(\frac{k^2}{2}\ln^2(\sigma)\right) \tag{5}$$

A simple combination with equation 5 gives a relationship between M_k and the log-normal parameters σ_g, R_g and N:

$$N = M_0 \tag{6}$$

$$R_g = \left(\frac{M_3^4}{M_6 M_0^3}\right)^{1/6} \tag{7}$$

$$\sigma_g = \exp\left(\frac{1}{3}\sqrt{\ln\left(\frac{M_0 M_6}{M_3^2}\right)}\right) \tag{8}$$

4. Moment methods and Aerosol dynamics

For aerosol with many monomers, it is possible to modelize the aerosol size distribution by a continuous function n relative to mean radius r_p. The general dynamical equation is given by *Friedlander* [1977]:

$$\frac{\partial n(r_p)}{\partial t} = (f_{convection} + f_{diffusion} + f_{coagulation} + f_{growth} + f_{sources/sink} + f_{external})(n(r_p)) \tag{9}$$

This equation can be integrated in terms of moments of the distribution as:

$$\frac{\partial M_k}{\partial t} = (f_{convection} + f_{diffusion} + f_{coagulation} + f_{growth} + f_{sources/sink} + f_{external})(M_k) \tag{10}$$

The aerosol dynamics are modeled as described by *Whitby et al.* [1991]; *Binkowski and Shankar* [1995]; *Ackermann et al.* [1998]; *Binkowski and Roselle* [2003] with notable differences: (1) We chose to integrate 3 moments (0, 3 and 6th) as prognostic variables. This procedure permits us to keep all parameters of the modal distribution variable. (2) Different sets of parameterization of sulfate nucleation and inorganic chemistry solvers are given. (3) The aerosol module is coupled on-line with meteorological fields and chemical species (organic condensation). (4) Sedimentation is integrated analyticaly

for all moments. (5) Surface exchange is coupled to a mesoscale atmosphere/biosphere model (section 5).

One can note that the moments of order 0 and 3 are well known ; the integration of $M_k = \int_0^\infty r_p^k n(r_p) dr_p$ gives for $M_{0,i} = N_i$ where N_i is the total concentration of particles for mode i and $M_{3,i} = \frac{3}{4\Pi} V_i$ is a direct function of the total volume of mode i.

4.1. Coagulation

4.1.1. General description Aerosol size distribution evolves by collision between particles, leading to coagulation process. Numerical cost of coagulation treatment is expensive but less expensive when a log-normal approach is used.

Several assumptions has been made to solve the binary coagulation: (1) A collision between two particles forms a new particle (2) The new particle is spherical (3) The new volume is equal to the sum of both initial particle volumes. Moments of the new particle formed after collision of particles of respective radius r_{p1} and r_{p2} is

$$r_{p12}^k = (r_{p1}^3 + r_{p2}^3)^{\frac{k}{3}} \tag{11}$$

It is necessary to consider coagulation as a transfer process of particles in the lognormal distribution: to update the moment evolution due to coagulation, we first consider the loss in moment due to extinction of both initial particles r_{p1} and r_{p2} (term $(r_{p1}^k + r_{p2}^k)$), and the supply of moment due to the creation of a new particule r_{p12} (term r_{p12}^k). The coagulation process can be integrated:

$$\begin{aligned} \frac{\partial M_k}{\partial t} &= \frac{1}{2} \int_0^\infty \int_0^\infty r_{p12}^k \beta(r_{p1}, r_{p2}) n(r_{p1}) n(r_{p2}) dr_{p1} dr_{p2} \\ &- \frac{1}{2} \int_0^\infty \int_0^\infty (r_{p1}^k + r_{p2}^k) \beta(r_{p1}, r_{p2}) n(r_{p1}) n(r_{p2}) dr_{p1} dr_{p2} \end{aligned} \tag{12}$$

with $\beta(r_{p1}, r_{p2})$ representing the coagulation rate between particles r_{p1} and r_{p2} in

$cm^3.s^{-1}$.

For the particular case of $N = 2$, different modes i and j ($N > 2$ is an extrapolation of results below), we obtain from 12 and 11:

$$\frac{\partial M_k}{\partial t} = \frac{1}{2}\int_0^\infty \int_0^\infty (r_{p1}^3 + r_{p2}^3)^{\frac{k}{3}} \beta(r_{p1}, r_{p2})(n_i + n_j)(r_{p1})(n_i + n_j)(r_{p2}) dr_{p1} dr_{p2}$$
$$-\frac{1}{2}\int_0^\infty \int_0^\infty (r_{p1}^k + r_{p2}^k) \beta(r_{p1}, r_{p2})(n_i + n_j)(r_{p1})(n_i + n_j)(r_{p2}) dr_{p1} dr_{p2} \quad (13)$$

It is easy to solve terms of equation 13 with the following convention: (1) When two particles collide in the same mode (intra-modal coagulation), the new one stays in this mode. (2) When two particles of different modes collide (inter-modal coagulation), the new one is in the mode with largest radius (here j). The second convention implies for the inter-modal coagulation that each particle of the lowest mode is transferred into the largest one. Nevertheless, the intra-modal coagulation of the lowest mode (i) is able to reach beyond the largest mode (j). As a consequence, we use an hybrid approach discussed by *Ackermann et al.* [1998]. First, the model resolves the intersection diameter (d_{eq}) of both modes, with the equation:

$$\ln\left(\frac{N_i \ln \sigma_i}{N_j \ln \sigma_j}\right) = \frac{(\ln d_{eq} - \ln d_{pi})^2}{2\ln^2 \sigma_{gi}} - \frac{(\ln d_{eq} - \ln d_{pj})^2}{2\ln^2 \sigma_{gj}} \quad (14)$$

At the end of the time-step, particles of the lowest mode (Aitken mode) with diameter greater than d_{eq} are transfered into the largest one (Accumulation mode).

4.1.2. Coagulation rate Coagulation is represented by an harmonic function which is an average between both coagulation limit regimes : 'free- molecular' and 'near continuum' [*Whitby et al.*, 1991]. Knudsen number defined by $Kn = \frac{\lambda}{r_p}$ permits to define the nature of the relationship between atmospheric gas and the particle. For

$Kn < 0.1$, the particle is in a continuous fluid (continuum regime), whereas for $Kn > 10$ the particle moves as a gas molecule (free molecular regime).

- Free molecular regime $Kn > 10$

  In this regime, *Friedlander* [1977] gave the expression of coagulation rate as:

$$\beta^{fm}(r_{p1}, r_{p2}) = \left(\frac{6kT}{\rho_p}\right)^{\frac{1}{2}} \left(\frac{1}{r_{p1}^3} + \frac{1}{r_{p2}^3}\right)^{\frac{1}{2}} (r_{p1} + r_{p2})^2 \tag{15}$$

  To integrate this equation, we need to make the same assumption as in *Lee et al.* [1984]:

$$\left(\frac{1}{r_{p1}^3} + \frac{1}{r_{p2}^3}\right)^{\frac{1}{2}} \approx \left(\frac{1}{r^{\frac{3}{2}_{p1}}} + \frac{1}{r^{\frac{3}{2}_{p2}}}\right) \tag{16}$$

  Now the equation 15 is written on the form:

$$\widetilde{\beta}^{fm}(r_{p1}, r_{p2}) = \left(\frac{6k_BT}{\rho_p}\right)^{\frac{1}{2}} \left(r_{p1}^{\frac{1}{2}} + 2\frac{r_{p2}}{r_{p1}^{\frac{1}{2}}} + \frac{r_{p2}^2}{r_{p1}^{\frac{3}{2}}} + \frac{r_{p1}^2}{r_{p2}^{\frac{3}{2}}} + 2\frac{r_{p1}}{r_{p2}^{\frac{1}{2}}} + r_{p2}^{\frac{1}{2}}\right) \tag{17}$$

  With this assumption, we can compute the variation of the moment due to coagulation process. But it is clear that this approximation is valid only in a short range of particle radius. To minimize the limitation of the approximation, a correction factor is definied as (for the mode i and k^{th} moment) :

$$b_{(6,i),intra} = \frac{\int_0^\infty \int_0^\infty r_{p1}^6 \beta^{fm} n_i(r_{p1}) n_i(r_{p2}) dr_{p1} dr_{p2}}{\int_0^\infty \int_0^\infty r_{p1}^6 \widetilde{\beta}^{fm} n_i(r_{p1}) n_i(r_{p2}) dr_{p1} dr_{p2}} \tag{18}$$

  These factors are tabulated in function of the log-normal parameters. Finally, we obtain:

$$\left(\frac{\partial M_{6,i}}{\partial t}\right)_{intra} \approx -b_{6,i,intra} \int_0^\infty \int_0^\infty r_{p1}^6 \widetilde{\beta}^{fm} n_i(r_{p1}) n_i(r_{p2}) dr_{p1} dr_{p2} \tag{19}$$

- Near-continuum regime $Kn < 1$

  For particles larger than their free mean path λ, *Friedlander* [1977] suggested the following expression for the coagulation rate:

$$\widetilde{\beta}^{nc}(r_{p1}, r_{p2}) = 4\Pi(D_{p1} + D_{p2})(r_{p1} + r_{p2}) \tag{20}$$

  where $D_p = (k_B T Cc/6\Pi\mu r_p)$,

  the Cunningham coefficient $Cc = 1 + Kn(a + b\exp(-c/Kn))$, with a=1.126; b=0.42 and c= 0.87.

  Equation 20 cannot be integrated analytically. If we consider only the continuum/near-continuum regime, we can approximate Cc as:

$$Cc \approx 1 + A^{nc'} Kn \tag{21}$$

  with $A^{nc'} = 1.392 Kn^{0.0783}$. After substitution, equation 20 becomes:

$$\widetilde{\beta}^{nc}(r_{p1}, r_{p2}) = \frac{2k_B T}{3\mu}\left(2 + \lambda A_i^{nc'}\left(\frac{1}{r_{p1}} + \frac{r_{p2}}{r_{p1}^2}\right) + \lambda A_j^{nc'}\left(\frac{1}{r_{p2}} + \frac{r_{p1}}{r_{p2}^2}\right) + \frac{r_{p1}}{r_{p2}} + \frac{r_{p2}}{r_{p1}}\right) \tag{22}$$

  As previously, correction factor can be considered. Nevertheless, the approximation used is precise enough in the continuum/near-continuum regime to be exempted.

- Generalization of Brownien Coagulation:

  Seinfeld and Pandis [1997] developed a general formulation for the coagulation rate $\beta(r_{p1}, r_{p2})$ using *Fuchs* [1964] formulation and a Cunningham coefficient due to *Philips* [1975]. But the expression is too complicated to be integrated in a log-normal distribution approach. That is why *Whitby et al.* [1991] proposed an alternative solution to compute all coagulation coefficients averaging previously expression of free-molecule and near continuum regime as:

$$\frac{\partial M_k}{\partial t} \approx \frac{(\frac{\partial M_k}{\partial t})^{fm}(\frac{\partial M_k}{\partial t})^{nc}}{(\frac{\partial M_k}{\partial t})^{fm} + (\frac{\partial M_k}{\partial t})^{nc}} \tag{23}$$

4.2. Gas-Particles conversion

Pre-existing particles grow by gaseous transfer upon their surface. A second way of gaseous-particles transfer is related to the formation of new particles by nucleation.

Just after the emission of a combustion particle, some of the gaseous species fix on the aerosol surface as an adsorption process. When these atmospheric molecules are either in sufficient number or on aerosol site with low curve radius, a phase change appears. At this stage, adsorption classical formalism on dry surface is not applicable. If the surface film is composed by an unique constituant in balance with the gas phase, when the atmospheric concentration of the constituant increases, molecules condense upon the aerosol surface to restore the thermodynamic balance.

The condensation process is discontinuous: the partial pressure needs to exceed a critical step to allow the phase change. In this case, the aerosol surface is crucial to transfer gaseous molecules into aerosol by condensation. The absorption process needs to have a pre-existing liquid film at the aerosol surface. The problem becomes different: as soon as a quantity of a species appears in gaseous phase, some molecules are transfered into particle phase by thermodynamical balance. In this model, we assume the aerosol is old enough to have a short liquid film at the surface. So, absorption has been retained as the dominant process of aerosol growth.

Gaseous species that interact with aerosol phase are from two different categories: mineral and organic species. Mineral species are fundamental to predict the condensation of water H_2O and thus the aerosol growth. Organic species include a large number

of different species with particular specificity of solubility, saturation vapor pressure and hearthless. The organic aerosol fraction is able to modify the aerosol hygroscopic specificity. It is necessary to distinguish the organic matter issued from urban and rural areas. The first one is mainly primary (emitted) and hydrophobic whereas the second one is mainly secondary (condensed) and hydrophilic [*Saxena et al.*, 1995].

4.2.1. Growth Processing Several parameters, such as temperature, relative humidity, total aerosol surface and the condensation matter rate determine which one is the principal growth factor of the aerosol. *Whitby et al.* [1991] gave the growth rate of the k^{th} moment relative to i mode as:

$$\frac{\partial M_{k,i}}{\partial t} = \frac{2k}{\Pi} \int_0^\infty r_p^{k-3} \Psi_p(r_p) n_i(r_p) dr_p \tag{24}$$

where Ψ_p is the condensation law on particles ($\mu m^3.s^{-1}$). Ψ_p can be separated in a Ψ_T and Ψ respectively independant and dependant on particle size.

$$\Psi_p = \Psi_T.\Psi \tag{25}$$

Equation 24 can be written as:

$$\frac{\partial M_{k,i}}{\partial t} = \frac{2k}{\Pi} \Psi_T I_{k,i} \tag{26}$$

with

$$I_{k,i} = \int_0^\infty r_p^{k-3} \Psi(r_p) n_i(r_p) dr_p \tag{27}$$

and

$$\Psi_T = \frac{m_w.(P_l - P_{surf,l})}{\rho_l RT} \tag{28}$$

where m_w is the molar mass of species l, P_l the partial pressure of species l, $P_{surf,l}$ the pressure of species l at the particle surface, ρ_l the volumic mass of l and T the

ambient temperature of the system (the aerosol is suposed to be in thermal equilibrium with its environment). $\Psi(r_p)$ is the size contribution with two asymptotic forms:

- Free molecular regime;

$$\Psi^{fm} = \pi\alpha\overline{c}r_p^2 \tag{29}$$

where α is the accomodation coefficient, $\overline{c}$ the kinetic velocity of vapor molecules ($\overline{c} = \sqrt{8RT/\pi m_w}$). Integration of equation 29 gives:

$$I_{k,i}^{fm} = \pi\alpha\overline{c}M_{k-1,i} \tag{30}$$

- Near continuum regime;

$$\Psi^{nc} = 4\pi D_v r_p \tag{31}$$

where D_v the diffusivity of species l in the air. Integration of equation 31 gives:

$$I_{k,i}^{nc} = 4\pi D_v M_{k-2,i} \tag{32}$$

Finally, with the same average as for coagulation we can approximate the general form of $I_{k,i}$ as:

$$I_{k,i} = \frac{I_{k,i}^{fm} I_{k,i}^{nc}}{I_{k,i}^{fm} + I_{k,i}^{nc}} \tag{33}$$

Pratsini [1988] estimated that this kind of procedure to average growth process is a very good approximation in the transitional regime. In our model, we assume thermodynamical equilibrium ($P_l = P_{surf,l}$)) in equation (28). We calculate $\delta\Psi_p$ as a diagnostic at the end of the timestep for use in equation (24).

4.2.2. Nucleation To activate the nucleation process of aerosol, it is necessary to have the partial vapor pressure of gas species greater than associated saturated vapor pressure. Nevertheless there is few knowledge about nucleation of organic matter. In this

model, only the sulfur nucleation is considered. We choose the *Kulmala et al.* [1998] parameterization for its consistance with the classical theory of binary homegeneous nucleation [*Wilemski*, 1984] and for taking into account the hydratation effect. The nucleation rate is parameterized as:

$$J = \exp\left(25.1289N_{sulf} - 4890.8\frac{N_{sulf}}{T} - \frac{1743.3}{T} - 2.2479\delta N_{sulf}RH + 7643.4\frac{x_{al}}{T} - 1.9712\frac{x_{al}}{RH}\right) \tag{34}$$

with $x_{al} = 1.2233 - \frac{0.0154RA}{RA+RH} + 0.0102\ln(N_{av}) - 0.0415\ln(N_{wv}) + 0.0016T$ the molar fraction of H_2SO_4 in the critical nucleus (stable);

N_{av} and N_{wv} respectively the concentration of sulfuric acid vapor and water vapor in cm^{-3};

T the atmospheric temperature (K), RA and RH absolute and relative humidity.

$N_{sulf} = \ln\left(\frac{N_a}{exp(-14.5125+0.1335T-10.5462RH+1958.4(RH/T))}\right)$ is the logarithm ratio between N_a (ambiant concentration of sulfur acid in cm^{-3}) and $N_{a,c}$ the concentration sulfur acid need to reach a nuclation rate of $J = 1cm^{-3}.s^{-1}$; and $\delta = 1 + \frac{T-273.15}{273.15}$. $N_{a,c}$ can be given by:

$$N_{a,c} = \exp(-14.5125 + 0.1335T - 10.5462RH + 1958.4(RH/T)) \tag{35}$$

4.2.3. Mineral Thermodynamic balance In this version, two sets of mineral thermodynamical equilibrium has been introduced for the prediction of the balance between aerosol and gas phases of the system NH_3- SO_4-HNO_3-H_2O. The first parameterization is ARES, a revised version of MARS [*Saxena et al.*, 1986], developed by *Binkowski and Shankar* [1995]. The second parameterization introduced is ISORROPIA from *Nenes et al.* [1998].

4.2.4. Heterogenous chemistry The aerosol phase can modify the gaseous composition by heterogeneous and multiphase reactions [*Ravishankara*, 1997]. Following *Jacob* [2000], we introduced the minimal set of reactions which is presented here with their associated uptake coefficients λ to improve the ozone model:

$$HO_2 \rightarrow 0.5H_2O_2 \qquad \lambda = 0.2 \tag{36}$$

$$NO_3 \rightarrow HNO_3 \qquad \lambda = 10^{-3} \tag{37}$$

$$NO_2 \rightarrow 0.5HNO_3 + 0.5HONO \qquad \lambda = 10^{-4} \tag{38}$$

$$N_2O_5 \rightarrow 2HNO_3 \qquad \lambda \in [0.01, 1] \tag{39}$$

The first order rate constant for gas heterogeneous loss onto particles is given by:

$$ka = \sum_k \left(\frac{d_k}{2D_g} + \frac{4}{\nu\lambda} \right)^{-1} A_k \tag{40}$$

with d_k the particle diameter (m), D_g the reacting gas molecular diffusivity ($m^2.s^{-1}$), μ the mean molecular velocity ($m.s^{-1}$), A_k the total surface area of mode k and λ the uptake coefficient of reactive species.

4.2.5. Organic condensation In the troposphere, Volatil Organic Compounds (VOCs) are mainly oxidized by OH radical, NO_3 and O_3. Some of these products have a very low saturated vapor pressure to be absorbed and form SOA. To take into account correct condensation process we need to restore thermodynamical balance for all species. If it is done for mineral species, it appears unrealistic for organic due to the important number of species. For *Pandis et al.* [1992], these oxydation products are accumulated in gaseous phase since they exceed their saturated vapor pressure and are able to condense on pre-existing aerosols. With this aim, some new chemical schemes, such as CACM

[*Griffin et al.*, 2002a] distinguish VOCs products in accordance with their capability to condense on the aerosol phase.

To treat absorption conversion of organic species to SOA (Secondary Organic Aerosol) it is common to use partition coefficients [*Pankow*, 1994] given by chamber measurements. Here we use *Schell et al.* [1998] and *Moucheron and Milford* [1996] partition coefficients for their compatibility with COV used in the RACM [*Stockwell et al.*, 1997] scheme. Then, a new set of chemical reactions has been added to the RACM gas phase (table 1).

SOA has been separated into SOAA (anthropic origin) and SOAB (biotic origin).

To take into account the particle size upon SOA condensation, we can use the previous integrated form of $I_{k,i}$ given by equation 33.

$$\frac{\partial M_{3,i}}{\partial t} = \frac{3\Delta SOA.I_{3,i}}{4\pi\rho_l} \tag{41}$$

with ΔSOA the fraction of SOA produced by the reaction scheme of table 1 in $kg.cm^{-3}.s^{-1}$. It is clear that this kind of SOA condensation parameterization is inadequate to reproduce a precise concentration of SOA in the aerosols. In the future, a thermodynamical approach similar to that of *Pun et al.* [2002] will be considered. **Table 1.**

4.3. Sedimentation - Dry deposition

Dry deposition and sedimentation of aerosols are driven by the Brownian diffusivity:

$$D_p = \left(\frac{kT}{6\pi\nu\rho_{air}r_p}\right) C_c \tag{42}$$

and by the gravitational velocity:

$$V_g = \left(\frac{2g}{9\nu}\left(\frac{\rho_{p,i}}{\rho_{air}}\right) r_p^2\right) C_c \tag{43}$$

where k is the Bolzmann constant, T the ambiant temperature, ν the air kinematic velocity, ρ_{air} the air density, g the gravitational acceleration, $\rho_{p,i}$ the aerosol density of mode i, and $C_c = 1 + 1.246\frac{\lambda_{air}}{r_p}$ the gliding coefficient. These expressions need to be averaged on the k^{th} moment and mode i as:

$$\hat{X} = \frac{1}{M_{k,i}} \int_{-\infty}^{\infty} X r_p^k n_i (\ln r_p) d(\ln r_p) \tag{44}$$

where X represents either D_p or v_g. After integration, we obtain for brownian diffusivity:

$$\hat{D}_{p_{k,i}} = \tilde{D}_{p_{g,i}} \left[\exp\left(\frac{-2k+1}{2} \ln^2 \sigma_{g,i} \right) + 1.246 K n_g \exp\left(\frac{-4k+4}{2} \ln^2 \sigma_{g,i} \right) \right] \tag{45}$$

with $\tilde{D}_{p_{g,i}} = \left(\frac{kT}{6\pi\nu\rho_{air} R_{g,i}} \right)$

and for gravitational velocity:

$$\hat{Vg}_{p_{k,i}} = \tilde{Vg}_{p_{g,i}} \left[\exp\left(\frac{4k+4}{2} \ln^2 \sigma_{g,i} \right) + 1.246 K n_g \exp\left(\frac{2k+4}{2} \ln^2 \sigma_{g,i} \right) \right] \tag{46}$$

with $\tilde{Vg}_{p_{g,i}} = \left(\frac{2g\rho_{p,i}}{9\nu\rho_{air}} R_{g,i}^2 \right)$

4.3.1. Dry Deposition According to *Seinfeld and Pandis* [1997] and using the resistance concept of *Wesely* [1989], aerosol dry deposition velocity for the k^{th} moment and mode i is:

$$\hat{v}_{d_{k,i}} = (r_a + \hat{r}_{d_{k,i}} + r_a \hat{r}_{d_{k,i}} \hat{Vg}_{p_{k,i}})^{-1} + \hat{Vg}_{p_{k,i}} \tag{47}$$

where surface resistance $\hat{r}_{d_{k,i}}$ is given by

$$\hat{r}_{d_{k,i}} = \left[(\hat{Sc}_{k,i}^{-2/3} + 10^{-3/\hat{St}_{k,i}}) \left(1 + 0.24 \frac{w_*^2}{u_*^2} \right) u_* \right]^{-1} \tag{48}$$

Schmidt and Stockes number are respectively equal to $\hat{Sc}_{k,i} = \nu / \hat{D}_{p_{k,i}}$ and $\hat{St}_{k,i} = (u_*^2 / g\nu)\hat{v}_{d_{k,i}}$. One can observe that the friction velocity u_* and the convective velocity w_* depend on meteorological and surface conditions.

4.3.2. Sedimentation For sedimentation process, we can use the above parameterization of $\hat{Vg}_{p_{k,i}}$. When vertical resolution is high, it is necessary to use a classical time splitting to compute sedimentation fluxes. It can be noted that the sedimentation / deposition processing modifies the particle distribution with an important loss of large particles in comparison to the small ones. After integration of the three moments, the distribution does not preserve the log-normal shape. If we consider after sedimentation processing the distribution as log-normal, the reconstruction of log-normal parameters σ, R_g induces a decrease of σ and an increase of R_g. The variation of σ is stronger than the R_g one. Nevertheless, in nature sedimentation process must decrease simultaneously σ and R_g. Therefore, we cannot consider the integration of the three moments to solve this problem. Two choices are possible:

- Sedimentation process with σ fixed : $M_{6,i}$ can be computed by maintaining σ equal to the previous values:

$$M_{6,i} = M_{0,i} \left(\frac{M_{3,i}}{M_{0,i}} \right)^{1/3} \exp\left(-3/2 \log(\sigma_g)^2\right)^6 \exp\left(18 \log(\sigma_g)^2\right) \tag{49}$$

- Sedimentation process with R_g fixed : A simple combination of $M_{k,i}$ gives $M_{6,i}$ in function of $M_{0,i}$, $M_{3,i}$, and $R_{g,i}$ as:

$$M_{6,i} = \frac{M_{3,i}^4}{R_{g,i}^6 M_{0,i}^3} \tag{50}$$

To decrease σ and R_g, a solution is to consider alternatively both treatment of $M_{6,i}$ for each time step.

5. IOP2b of Escompte Campaign using Meso-NH-C model

5.1. Three dimensional coupling into Meso-NH-C model

Meso-NH is a meteorological model jointly developed by CNRM (Meteo France) and Laboratoire d'Aérologie (CNRS) [*Lafore et al.*, 1998]. Objectives are to determine most various atmospheric processes and to tackle complex real or ideal atmospheric phenomena. Meso-NH allows simulations from small scale (LES type) to synoptic scale (horizontal resolution ranging from a few meters to several tens of kilometers) and can be run in a two-way nested mode involving up to 8 nesting stages. Different sets of parameterizations have been introduced for convection [*Kain and Fritsch*, 1993] and [*Bechtold et al.*, 2001], cloud microphysics [*Cohard and Pinty*, 2000b], turbulence [*Bougeault and Lacarrre*, 1989], surface thermodynamic exchanges (biosphere atmosphere interactions ISBA [*Noilhan and Mahouf*, 1995], urban-atmosphere interactions TEB [*Masson*, 2000]), lightning processes [*Barthe et al.*, 2004]. Meso-NH-C model is an on-line coupling between Meso-NH and several chemical modules described by *Suhre et al.* [1998], *Mari et al.* [2000] and *Tulet et al.* [2003].

Two sets of aerosol parameterizations have been coupled into the chemical scheme of Meso-NH-C. The first one (ORganic Inorganic Sectional Aerosol Model (ORISAM) developed by *Bessagnet et al.* [2004] and introduced in Meso-NH-C by *Cousin et al.* [2004] is a bin parameterization model. The second one (ORILAM), described above, use a three moments log-normal parameterization (number, mass composition and standard deviation are explicit). These aerosol modules use the same core chemical system (ReLACS [*Crassier et al.*, 2000]) adding a range of 8 aerosol variables such as (OC (primary organic aerosol), BC (black carbon) , $SOAA$ (secondary anthropic

organic aerosol) , $SOAB$ (secondary biogenic organic aerosol), H_2O (water), NH_3 (ammonium), NO_3 (nitrates), SO_4 (sulfates). The version of ORISAM used in *Cousin et al.* [2004] simulation has 4 bins (2 for each aerosol mode), for a total of 32 aerosol prognostic variables. The log-normal approach uses the set of aerosol species for each mode. For the simulations, two log-normal modes have been used in ORILAM (dust mode has been desactivated) with the same aerosol species as ORISAM (OC, $BC, SOAA, SOAB, H2O, H3, NO3, SO4$) for a total of 20 aerosol prognostic variables (16 plus M_0 and M_6 each mode). Indeed, ORISAM gives a fine information of the aerosol composition in each bin but with a large number of prognostic variables and a pre-defined distribution structure (size and dimensional position of each bin are fixed in time), whereas ORILAM gives an aerosol composition in each mode but with fewer prognostic variables and an evolutive spectral distribution.

5.2. IOP2b of the Escompte Campaign

Escompte is a European program designed to establish an exhaustive database for the development and the validation of numerical air pollution models (*Cros et al.* [2004]). The region of Marseille / Fos / Berre (south east of France) is characterized by a complex topography subject to channeling effects and sea-breeze circulations, with strong industrial, urban and biogenic emission sources. This region has been selected for its frequent summer photochemical pollution episodes. Four Intensive Observation Periods (IOP) have been identified. The most significant one is IOP 2a/b, a 6-day complex pollution episode. *Cousin et al.* [2005] examined the interaction between regional and urban pollution and gave a complete analysis of gaseous redistribution and pollution enhancement during the IOP2b using the Meso-NH-C model.

In particular, June 24^{th} is characterized in the Marseille-Fos-Berre region by a sea-breeze circulation embedded in a synoptic northerly flow [*Cousin et al.*, 2005]. After penetrating inland, winds turn to the south-west, driving pollutant plume from the Berre pond to the Durance Valley. During June 24^{th} air temperature was about 15 to $18°C$ in the morning, increasing during the day to $28 - 30°C$. Relative humidity was high in the morning and in the evening (about 90%).

5.3. Model configuration

Two-way nested grid simulations were performed. The large domain (9 km resolution) between $40.8°N$ and $47°N$ in latitude and $1.06°E$ and $10.02°E$ in longitude, incorporates large pollution source regions such as Barcelona, Marseille, Lyon and the Po valley (Italy). The embedded ESCOMPTE small domain (3 km resolution) centered at Marseille and the Berre pond is located between latitudes $42.7°N$ and $44.3°N$ and longitudes $4.22°E$ and $6.42°E$. The vertical resolution is composed of 54 vertical levels, 40 of them being located in the boundary layer between the surface and 2500 m. Initialization and lateral boundary conditions of the large domain have been given by the global nested chemical transport model MOCAGE [*Dufour et al.*, 2004] for the chemical gaseous part and by the operational meteorological model ARPEGE [*Courtier et al.*, 1991] for atmospheric dynamics. Top boundary gravity waves have been filtered by an absorbing layer at 8000 meters.

For carbonaceous primary aerosol, the CO fields given by MOCAGE were used to derive BC and OC initial fields by adapted scaling obtained by average BC/CO and OC/CO surface concentration ratios. Other aerosol species were initialized to a zero

value. An anthropogenic emission inventory with a resolution of 9 km, has been used for gas phase from GENEMIS database [*Wickert et al.*, 1999]. For emission of carbonaceous primary aerosols (OC, BC) we extrapolate the BC and OC ESCOMPTE daily emission [*Liousse*, 2005] by an hourly CO variation to obtain an hourly variation of BC and OC emissions. Concerning sulphates, we introduce a primary emission of SO_4^{2-} with a ratio of 2% of total SO_x emitted in industrial combustion plumes, following *Kasibhatla et al.* [1997] and *Tan et al.* [2002].

Simulations for June 24^{th} begin on June 23^{rd} at 12.00 UTC with a a spin-up period of 12 hours. For mineral equilibrium, the ORILAM simulation chooses ARES parameterization whereas ORISAM uses ISORROPIA.

5.4. Comparison between measurements, ORILAM and ORISAM simulations

Four stations have been devoted to analyze aerosol chemical composition: an urban station (Marseille); an industrial station (Martigues), a rural station located in forest influenced by industrial plume (Dupail); a suburban station influenced by both urban and industrial pollution (Realtor) and a station at 800 meters in altitude, north of Marseille (Plan d'Aups). All aerosol measurements can be found in *Cachier et al.* [2005]. One can note that sulphate measurements were made with ionic chromatography. Ammonium and nitrate measurements have some uncertainties due to unuse of denuder (overestimation) and filter treatment (underestimation). POM and BC (Fig. 1) are provided from filter budget, otherwise the BC evolution has been measured with an aethalometer (Fig. 2). Another uncertainty concern PM 10 measurement (underestimation of the semi-volatile fraction), made by using a TEOM with an inlet warmed at 50 $^{\circ}C$ (Fig. 3). Nevertheless, the aerosol mass composition reveals that semi-volatile compounds do not exceed 10 %

[*Cachier et al.*, 2005].

Using this aerosol data base, *Cousin et al.* [2004] examine the aerosol composition simulated during IOP2b by MesoNH-C and ORISAM aerosol scheme. Dynamical and gaseous data comparisons can be found in the gaseous study of IOP2b [*Cousin et al.*, 2005]. We focus here to reproduce the same order of magnitude of aerosol composition observed during the IOP2b and simulated by ORISAM [*Cousin et al.*, 2004]. ORILAM and ORISAM simulation use the same initial condition, lateral boundary coupling, gaseous and aerosol emissions. But some light differences on simulated wind field has been observed due to the use of a more recent version of MesoNH-C in this study. This can explain the major differences between both simulations particularly in coastal area such as Marseille and Martigues where wind field is more variable. Indeed, this comparison confirms that ORILAM reproduces the results from the previously validated model ORISAM.

5.4.1. Mean aerosol composition Except for Martigues, one can observe in Fig. 1 an important underestimation of sulphate concentration. *Cousin et al.* [2004] assumes that it depends on the relative humidity underestimation observed in meteorological analysis used in our simulation. Dry air could affect the heterogeneous sulphate production. Another reason of sulphates under production could be explained by the DMS oxidation which is not integrated in these simulations. But this under production in some urban areas such as Marseilles is probably due to a local source non included in the emission database. The second large underestimation concerns nitrate. Neither ORILAM and ORISAM can reproduce the measured nitrate in aerosols. As for sulphate it could be attributable to low RH. Another reason could be that terrigeneous calcium carbonates not present in ISORROPIA and ARES, could react and neutralize $HNO3$

[*Dentener et al.*, 1996]; [*Tabazadeh et al.*, 1998]. *Cachier et al.* [2005] have shown results (from detailed impactor) where nitrate was almost uniquely found in the coarse fraction of the aerosol and probably attached to dust and sea-salt particles. This has been already evidenced by *Jacobson* [1999]. BC concentration is quite well reproduced by both ORILAM and ORISAM simulations; total BC primary emissions emitted during June 24^{th} seem to be correct for both location and quantity. Except for Plan d'Aups and Dupail, the order of magnitude for POM concentration is correctly reproduced. For plan d'Aups, Escompte's experimentalists do not understand the high values of POM measured whereas other species observed here are low; at this stage, modeling could not give more explanations. At Dupail, all aerosol constituents are underestimated. The complex location of Dupail could be affected by an industrial plume whereas the dynamic reproduction of Meso-NH indicates that the simulated industrial plume is located west of Dupail.

Figure 1.

5.4.2. Evolution of BC and $PM10$ concentration Figures 2 and 3 respectively display the comparison between ORILAM and ORISAM, for measurements of BC and $PM10$, with diurnal evolution during June 24^{th} at station Martigues (a), Realtor (b), Dupail (c), Plan d'Aups (d) and Marseille (e). One can observe a quite good order of magnitude for BC concentration with ORILAM and ORISAM (Fif. 2). Several pollution peaks and night low values have been correctly simulated in time in Plan d'Aups , Marseille and Dupail; Marseille, as a pure urban station, gives the best results. An inter-comparison between ORILAM and ORISAM gives similar evolution: ORILAM seems to be better at Marseille, Plan d'Aups and Martigues whereas ORISAM seem to be better at Dupail. This good reproduction of primary aerosol validates the BC emission evolution and the aerosol scheme. PM 10 concentrations are strongly underestimated.

This was expected since these models do not consider re-suspended particles and dust which is an important part of the total mass of PM 10. In addition, underestimation in Plan d'Aups increases by a bad reproduction of POM; at Marseilles it is increased by the sulphate underestimation; at Dupail both sulphate and POM. BC and $PM10$ evolutions are strongly influenced by the mixing layer thickness and the sea breeze regime; some results such as BC evolution show that MesoNH is able to reproduce correctly these mesoscale mixing and transport.

Figure 2.

Figure 3.

6. Conclusion and perspectives

This paper presents the ORILAM aerosol scheme. Due to its few number of aerosol variables this aerosol scheme has been developed for mesoscale and global atmospheric model. The use of three moments makes ORILAM able to reproduce a large number of aerosol distributions and their evolution in time and space (aerosol composition, mean radius and standard deviation of the distribution are explicit). Meso-NH-C and ORILAM/ORISAM coupling is one of the first on-line coupling concerning a non-hydrostatic mesoscale model, a complete chemical scheme and an aerosol module. It has been tested upon a coastal region during the IOP2b of the Escompte campaign. Results give an overall good agreement between observations and simulations, particularly for BC concentration. A 20 % underestimation of relative humidity (RH) simulated during the June 24th could explain the underestimation of nitrate and ammonium absorbed by aerosols [*Nenes et al.*, 1998] . Particle size distribution are well reproduced in the sub-micrometer range only. The next steps are to introduce dust emissions and in some extent, marine particles to further improve the prediction of $PM10$ concentrations and the accurate modeling of gas-particle interactions. Inter-comparison between

ORILAM and ORISAM schemes gives the same order of magnitude for several aerosol components; both have the same defaults and quality in their predictions. Nevertheless, due to few prognostic variables, the lognormal approach is cheaper in term of numerical cost: one lognormal mode is comparable to two bins of the sectional scheme.

The Escompte area is characterized by a large number of heterogeneities for pollutants: industrial and urban plumes are mixed and advected by marine breeze and catabatic flow. It reveals a great challenge to predict accurate RH and thus, the aerosol composition. The use of on-line simulations appear to be a good method to predict aerosol distribution in polluted coastal areas such as Marseille. Soon, a complete description of polluted layers [*Cousin et al.*, 2004] will be analyzed in term of composition and aerosol provenance. The principal way of ORILAM development will concern the hygroscopicity (or hydrophobicity) of organic compounds. An hydrophobic and hydrophilic module will be introduced and coupled to SOA as described in *Pun et al.* [2002]. Therefore, MesoNH/ORILAM will be able to predict CCN activation via a microphysics closure between the heterogeneous chemistry and the cloud schemes.

Acknowledgments. The authors greatly thank Dr C. Liousse and Mr. B. Guillaume for providing the Aerosol emission database. We also wish to thanks Dr. H. Cachier and F. Aulagnier for their aerosol data base and all the Escompte community for their works upon Marseille area during summer 2001. All computation for this work was done on the Meteo-France supercomputers.

References

Ackermann, I., H. Hass, M. Memmesheimer, A. Ebel, F. Binkowski, and U. Shankar, Modal aerosol dynamics model for Europe : development and first applications., *Atmospheric Environment*, *32(17)*, 2981–2999, 1998.

Barthe, C., G. Molini, and J. Pinty, Description and first results of an explicit electrical scheme in a 3d cloud resolving model, *Atmos. Res.*, *in press*, 2004.

Bechtold, P., E. Bazile, F. Guichard, P. Mascart, and E. Richard, A mass-flux convection scheme for regional and global models, *Quart. J. Roy. Meteor. Soc.*, *127*, 869–886, 2001.

Bessagnet, B., and R. Rosset, Fractal modelling of carbonaceous aerosols-application to car exhaust plumes, *Atmospheric Environment*, *35*, 4751–4762, 2001.

Bessagnet, B., A. Hodzic, R. Vautard, M. Beekmann, S. Cheinet, C. Honor, C. Liousse, and L. Rouil, Aerosol modeling with CHIMERE-Preliminary evaluation at the continental scale, *Atmospheric Environment*, *in press*, 2004.

Binkowski, F., and S. Roselle, Models-3 community multiscale air quality (cmaq) model aerosol component. 1. Model description, *J. Geophys. Res.*, *108*, D6, 2003.

Binkowski, F., and U. Shankar, The regional particulate model 1. Model description and preliminary results, *J. Geophys. Res.*, *100*, 26,191–26,209, 1995.

Bougeault, P., and P. Lacarrre, Parametrization of orography-induced turbulence in a meso-beta model, *Mon. Wea. Rev.*, *117*, 1872–1890, 1989.

Cachier, H., et al., Aerosol studies during the ESCOMPTE experiment : an overview., *Atmospheric Research*, *74*, 547–563, 2005.

Cohard, J., and J. Pinty, A comprehensive two-moment warm microphysical bulk scheme . ii : 2d experiments with a non hysrostatic model., *Quart. J. Roy. Meteor. Soc.*, *126*, 1843–1859, 2000b.

Courtier, P., C. Freydier, J. Geleyn, F. Rabier, and M. Rochas, The arpege project at meteo france, *Proceedings of the ECMWF seminar*, *7*, 193–231, 1991.

Cousin, F., C. Liousse, H. Cachier, B. Bessagnet, B. Guillaume, and R. Rosset, Aerosol modelling and validation during escompte 2001., *Atmospheric Environment*, *39*, 1539–1550, 2004.

Cousin, F., P. Tulet, and R. Rosset, Interaction between local and regional pollution during escompte 2001 : impact on surface ozone concentrations (iop2a and 2b)., *Atmospheric Research*, *74*, 117–137, 2005.

Crassier, V., K. Suhre, P. Tulet, and R. Rosset, Development of a reduced chemical scheme for use in mesoscale meteorological models, *Atmos. Environ.*, *34*, 2633–2644, 2000.

Cros, B., et al., The ESCOMPTE program : an overview., *Atmospheric Research*, *69,3-4*, 241–279, 2004.

Dentener, J., G. Carmichael, Y. Zhang, J. Lelieveld, and P. Crutzen, Role of mineral aerosol as a reactive surface in the global troposphere., *J. Geophys. Res.*, *101*, 22,869–22,889, 1996.

Dufour, A., M. Amodei, G. Ancellet, and V.-H. Peuch, Observed and modelled chemical weather during ESCOMPTE., *Atmospheric Research*, *in press*, 2004.

Friedlander, S., Smoke, Dust, and Haze, Fundamentals of aerosols dynamics, *Oxford University Press*, *2nd ed*, 1977.

Fuchs, N., The mechanism of aerosols, *Pergamon Press, Oxford*, 1964.

Griffin, R., D. Dabdub, M. Kleeman, M. Fraser, G. Cass, and J. Seinfeld, Secondary organic aerosol. 3. Urban/regional scale model of size-and composition-resolved aerosols., *J. Geophys. Res.*, *107(D17), 4334*, doi:10.1029/2001JD000,544, 2002.

Griffin, R., D. Dabdub, and J. Seinfeld, Secondary organic aerosol. 1. Atmospheric chemical mechanism for production of molecular constituents., *J. Geophys. Res.*, *107(D17), 4332*, doi:10.1029/2001JD000,541, 2002a.

Harrington, D., and S. Kreidenweis, Simulation of sulfate aerosol dynamics part ii. model intercomparion, *Atmos. Environ.*, *32*, 1701–1709, 1998.

Jacob, D., Heterogenous chemistry and tropospheric ozone, *Atmospheric Environment*, *34*, 2131–2159, 2000.

Jacobson, M., Development and application of a new air pollution modelling system-II. Aerosol module structure and design., *Atmospheric Environment*, *31*, 131–144, 1997.

Jacobson, M., Studying the effects of calcium and magnesim on size-distributed nitrate and ammonium with EQUISOLV II., *Atmospheric Environment*, *33*, 3635–3649, 1999.

Jacobson, M., R. Lu, R. Turco, and O. Toon, Development and application of a new air pollution modeling system - Part I : gas-phase simulations., *Atmospheric Environment*, *30*, 1939–1963, 1996.

Kain, J., and J. Fritsch, Convective parameterization for mesoscale models: The kain-fitsch scheme, *Meteo. Monographs*, *46*, 165–170, 1993.

Kasibhatla, P., W. Chameides, and J. S. John, A three-dimensional global model investigation of seasonal variations in the atmospheric burden of anthropogenic sulphate aerosols., *J. Geophys. Res.*, *102(D3)*, 3737–3759, 1997.

Kulmala, M., A. Laaksonen, and L. Pirjola, Parametrization for sulfuric acid / water nucleation rates., *J. Geophys. Res.*, *103, D7*, 8301–8307, 1998.

Lafore, J., et al., The meso-nh atmospheric simulation system. part i: adiabatic formulation and control simulations, *Ann. Geophys.*, *16*, 90–109, 1998.

Lee, K., H. Chen, and J. Gieseke, Log-normally preserving size distribution for brownian coagulation in the free-molecule regime, *Aerosol Sci. Technol.*, *3*, 1984.

Liousse, C. a. B. G., Development of fossil fuel carbonaceous aerosol emission inventories at

european, national and regional scales, paper in preparation for atmospheric environment., *Atmospheric Environment*, 2005.

Lurmann, F., A. Wexler, N. Pandis, S. Musara, N. Kumar, and J. Seinfeld, Modeling urban and regional aerosols. ii. application to california's south coast air basin for urban-scale air quality simulation models, *Atmospheric Environment*, *31*, 2695–2715, 1997.

Mari, C., D. Jacob, and P. Bechtold, Transport and scavenging of soluble gases in a deep convective cloud, *J. Geophys. Res.*, *105*, 22,255–22,263, 2000.

Masson, V., A physically-based scheme for the urban energy balance in atmospheric models., *Boundary-Layer Meteorology*, *94*, 357–397, 2000.

Meng, Z., D. Dabdub, and J. Seinfeld, Size-resolved and chemically resolved model of atmospheric aerosol dynamics., *J. Geophys. Res.*, *103*, 3419–3435, 1998.

Moucheron, M., and J. Milford, Development and testing of a process model for secondary organic aerosols., *Air and Waste Management Association, Nashville*, 1996.

Nenes, A., C. Pilinis, and S. Pandis, ISORROPIA : A new thermodynamic model for inorganic multicomponent atmospheric aerosols., *Aquatic Geochemistry*, *4*, 123–152, 1998.

Noilhan, J., and J. Mahouf, The isba land surface parametrisation scheme., *Global planetary Change*, *13*, 145–159, 1995.

Pai, P., K. Vijayaraghavan, and C. Seigneur, Particulate matter modeling in the los angeles basin using saqm-aero, *J. Air Waste Manage. Assoc.*, *50*, 32–42, 2000.

Pandis, S., R. Harley, G. Cass, and J. Seinfeld, Secondary organic aerosol formation and transport., *Atmospheric Environment*, *26A*, 2269–2282, 1992.

Pandis, S., A. Wexler, and J. Seinfeld, Secondary organic aerosol formation and transport-ii. predicting the ambient secondary organic aerosol size distribution., *Atmospheric Environment*, *27A*, 2403–2416, 1993.

Pankow, J., An absorption model of the gas/aerosol partitioning involved in the formation of secondary organic aerosol., *Atmospheric Environment*, *28*, 189–193, 1994.

Philips, W., Drag on small sphere moving throught a gas, *Phys. Fluids*, *18*, 1089–1093, 1975.

Pilinis, C., and J. Seinfeld, Continued development of a general equilibrium model for inorganic multicomponent atmospheric aerosols., *Atmospheric Environment*, *21*, 2453–2466, 1987.

Pratsini, S. E., Simultaneous aerosol nucleation, codensation, and coagulation in aerosol reactors, *J. Colloid Interface Sci.*, *124*, 416–417, 1988.

Pun, B., R. Griffin, C. Seigneur, and J. Seinfeld, Secondary organic aerosol. 2. Thermodynamic model for gas/partitioning of molecular constituents., *J. Geophys. Res.*, *107(D17), 4333*, doi:10.1029/2001JD000,542, 2002.

Raes, F., A. Saltelli, and R. V. Dingenen, Modelling formation and growth of $h_2so_4 - h_2o$ aerosols: Uncertainty analysis and experimental evaluation., *J. Atmos. Sci.*, *23*, 759–772, 1992.

Ravishankara, A., Heterogeneous and multiphase chemistry in the troposphere., *Science*, *276*, 1058–1065, 1997.

Russell, A., and G. Cass, Verification of a mathematical model for aerosol nitrate and nitric acid formation and its use for control measure evaluation., *Atmospheric Environment*, *20*, 2011–2025, 1986.

Saxena, P., A. Hudischewskyj, C. Seigneur, and J. Seinfeld, A comparative study of equilibrium approaches to the chemical characterization of secondary aerosols, *Atmospheric Environment*, *20*, 1471–1483, 1986.

Saxena, P., L. Hildemann, and J. Seinfeld, Organics alter hygroscopic behavior of atmospheric particles, *J. Geophys. Res.*, *100*, 18,755–18,770, 1995.

Schell, B., I. Ackermann, H. Hass, and A. Ebel, Secondary organic aerosol modelling with made:

biogenic and anthropogenic contributions., *Procedings of Eurotrac 2 - WIT Press*, *2*, 638–642, 1998.

Seigneur, C., A. Hudischewskyj, J. Seinfeld, K. Whitby, E. Whitby, J. Brock, and H. Barnes, Simulation of aerosol dynamics: a comparative review of mathematical models., *Aerosol Sci. and Tech.*, *5*, 205–222, 1986.

Seinfeld, J., and S. Pandis, Atmospheric Chemistry and Physics, *Wiley interscience pub*, 1997.

Stockwell, W., F. Kirchner, M. Kuhn, and S. Seefeld, A new mechanism for regional atmospheric chemistry modeling, *J. Geophys. Res.*, *102*, 847–25, 879, 1997.

Suhre, K., et al., Physico-chemical modeling of the first aerosol characterization experiment (ace 1) lagrangian b, 1. a moving column approach, *J. Geophys. Res.*, *103*, 16,433–16,455, 1998.

Suhre, K., et al., Chemistry and aerosols in the marine boundary layer: 1-d modelling of the three ace-2 lagrangian experiments, *Atmospheric Environment*, *34*, 5079–5094, 2000.

Sun, Q., and A. Wexler, Modeling urban and regional aerosols-condensation and evaporation near acid neutrality, *Atmospheric Environment*, *32*, 3527–3531, 1998.

Tabazadeh, A., M. Jacobson, H. Singh, O. Toon, J. Lin, R. Chatfield, A. Thakur, R. Talbot, and J. Dibb, Nitric acid scavenging by mineral and biomass burning aerosols., *Geophysical Res. Let.*, *25*, 4185–4188, 1998.

Tan, Q., Y. Hang, and W. Chameides, Budget and export of anthropogenic SOx from East Asia during continental outflow conditions., *J. Geophys. Res.*, *107(D13)*, doi:10.1029/2001JD000,769, 2002.

Tsang, T., and A. Rao, Comparison of different numerical schemes for condensational growth of aerosols., *Atm. Sci. and Tech.*, *9*, 271–277, 1988.

Tulet, P., V. Crassier, F. Solmon, D. Guedalia, and R. Rosset, Description of the mesoscale

nonhydrostatic chemistry model and application to a transboundary pollution episode between northern france and southern england, *J. Geophys. Res.*, *108*, D1, 4021, 2003.

Wesely, M., Parametrizations of surface resistance to gaseous dry deposition in regional scale, numerical models, *Atmos. Environ.*, *23*, 1293–1304, 1989.

Wexler, A., F. Lurman, and J. Seinfeld, Modelling urban and regional aerosols, I. Model development., *Atmospheric Environment*, *28*, 531–546, 1994.

Whitby, E., and P. McMurry, Modal aerosol dynamics modeling., *Aerosol Sci. and Techn.*, *27*, 673–688, 1997.

Whitby, E., P. McMurry, U. Shankar, and F. Binkowski, Modal aerosol dynamics modeling., *Atm. Res. and Exposure Asses. Lab., U.S. Environ. Prot. Agency, Research Triangle Park, N.C.*, 1991.

Wickert, B., U. Schwartz, P. Blank, C. John, J. Kuhlwein, A. Obermeier, and R. Friedrich, Generation of an emission data base for europe 1994, *Proceedings of Eurotrac symposium 98*, *2*, 255–265, 1999.

Wilemski, G., Composition of the critical nucleus in multicomponent vapor nucleation., *J. Chem. Phys.*, *80*, 1370–1372, 1984.

Wilson, J. F. R., m^3 multi modal model for aerosol dynamics. in: Nucleation and atmospheric aerosol, *In: Nucleation and Atmospheric Aerosol, eds. M. Kulmala and P.E. Wagner. Elsevier Oxford, U.K.*, 1996.

Zhang, Y., C. Seigneur, J. Seinfeld, M. Jacobson, and F. Binkowski, A comparative review of algorithms used in air quality models., *Aerosol Sci. Technol.*, *31*, 487–514, 1999.

Zhang, Y., B. Pun, K. Vijayaraghavan, S. Wu, C. Seigneur, S. Pandis, M. Jacobson, A. Nenes, and J. Seinfeld, Development and application of the model of aerosol dynamics

reaction, ionization, and dissolution (madrid), *J. Geophys. Res.*, *109 (D01202)*, doi:10.1029/2003JD003,501, 2004.

P. Tulet, V. Crassier, F. Cousin, K. Suhre, R. Rosset, CNRM/GMEI 42 av G. Coriolis, 31057 Toulouse France (pierre.tulet@meteo.fr, vincent.crassier@oramip.org, couf@aero.obs-mip.fr, Karsten.Suhre@igs.cnrs-mrs.fr, rosr@aero.obs-mip.fr)

Received _____

This manuscript was prepared with AGU's LaTeX macros v5, with the extension package 'AGU^{++}' by P. W. Daly, version 1.6a from 1999/05/21.

Figure Captions

Figure 1. Average concentration of Black Carbon (BC), Particulate Organic Matter (POM), Nitrates (NO3), Ammonium (NH4) and Sulfates (SO4) on June 24 at : (a) Martigues, (b) Realtor, (c) Dupail, (d) Plan d'Aups and (e) Marseille (measurement in black, ORISAM simulation in dark grey and ORILAM simulation in light grey).

Figure 2. Average concentration of Black Carbon (BC), Particulate Organic Matter (POM), Nitrates (NO3), Ammonium (NH4) and Sulfates (SO4) on June 24 at : (a) Martigues, (b) Realtor, (c) Dupail, (d) Plan d'Aups and (e) Marseille (measurement in black, ORISAM simulation in dark grey and ORILAM simulation in light grey).

Figure 3. PM-10 time series (scale in $\mu g.m^{-3}$ at the left) on June 24 at: (a) Martigues, (b) Realtor, (c) Dupail, (d) Plan d'Aups and (e) Marseille (dark curve for measurement, squares for ORISAM simulation in dark grey and grey triangle for ORILAM simulation).

Tables

Kinetic constant	Chemical Reaction
2.171E+5/M*exp(-(+155.0/T))	HC5 + OH → 4.8 SOAA
2.096E+7/M*exp(-(+125.0/T))	HC8 + OH → 7.9 SOAA
2.453E+6/M*exp(-(-500.0/T))	OLT + OH → 3.8 SOAA
5.371E+6/M*exp(-(-500.0/T))	OLI + OH → 5.0 SOAA
2.950E+6/M*exp(-(-355.0/T))	TOL + OH → 7.1 SOAA
1.229E+7/M*exp(-(-355.0/T))	XYL + OH → 8.9 SOAA
6.366E+7/M	CSL + OH → 6.6 SOAA
5.482E+4/M*exp(-(-331.0/T))	ALD + OH → 2.4 SOAA
3.572E+7/M*exp(-(-444.0/T))	API + OH → 10.0*SOAB
5.048E+8/M*exp(-(-444.0/T))	LIM + OH → 10.0*SOAB

Table 1. With T the air temperature in K and M the concentration of air molecule in $molecules.cm^{-3}$ of RACM species [*Stockwell et al.*, 1997]

Figures

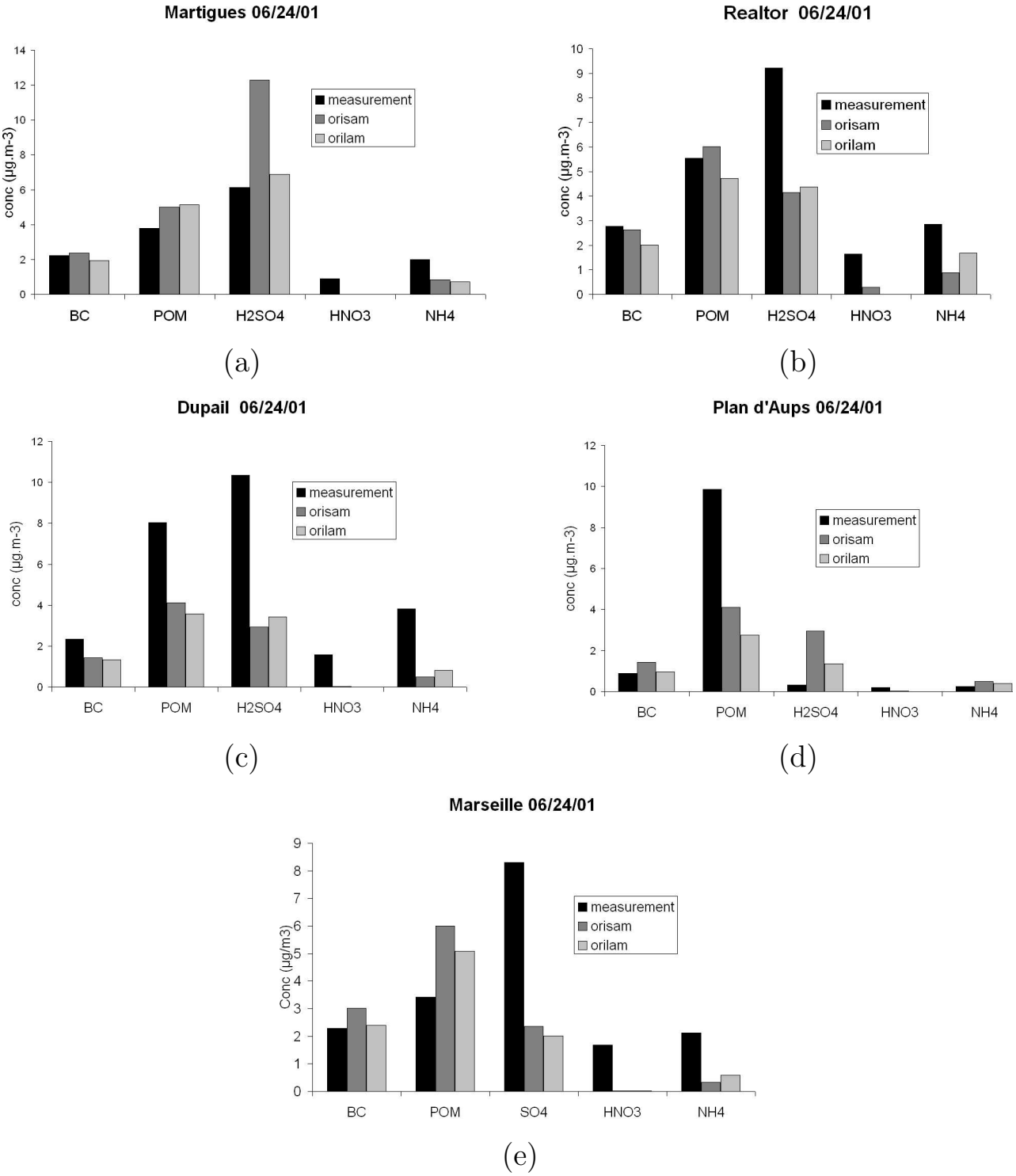

Figure 1:

Figure 1. Average concentration of Black Carbon (BC), Particulate Organic Matter (POM), Nitrates (NO3), Ammonium (NH4) and Sulfates (SO4) on June 24 at : (a) Martigues, (b) Realtor, (c) Dupail, (d) Plan d'Aups and (e) Marseille (measurement in black, ORISAM simulation in dark grey and ORILAM simulation in light grey).

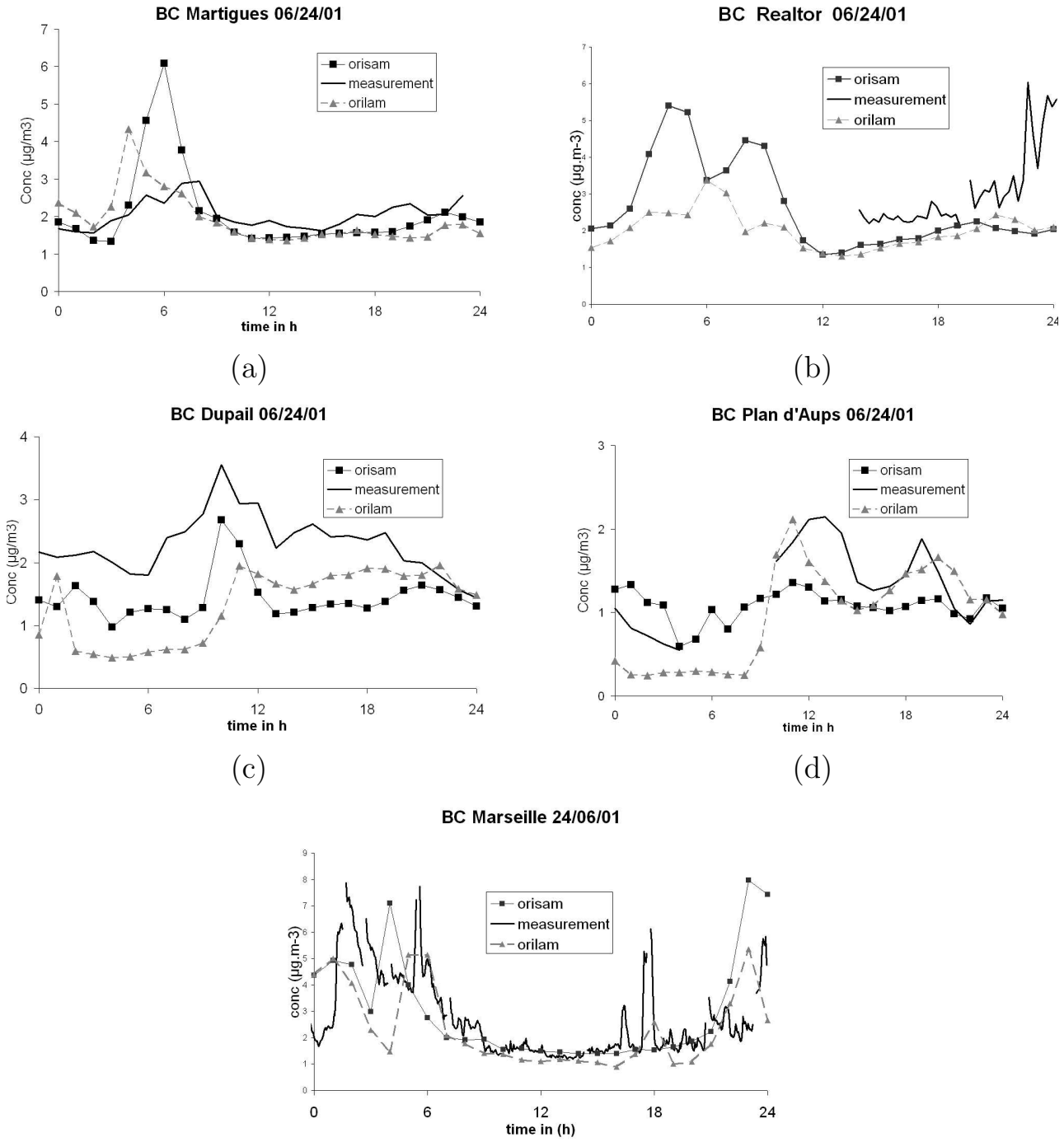

Figure 1:

Figure 2. Average concentration of Black Carbon (BC), Particulate Organic Matter (POM), Nitrates (NO3), Ammonium (NH4) and Sulfates (SO4) on June 24 at : (a) Martigues, (b) Realtor, (c) Dupail, (d) Plan d'Aups and (e) Marseille (measurement in black, ORISAM simulation in dark grey and ORILAM simulation in light grey).

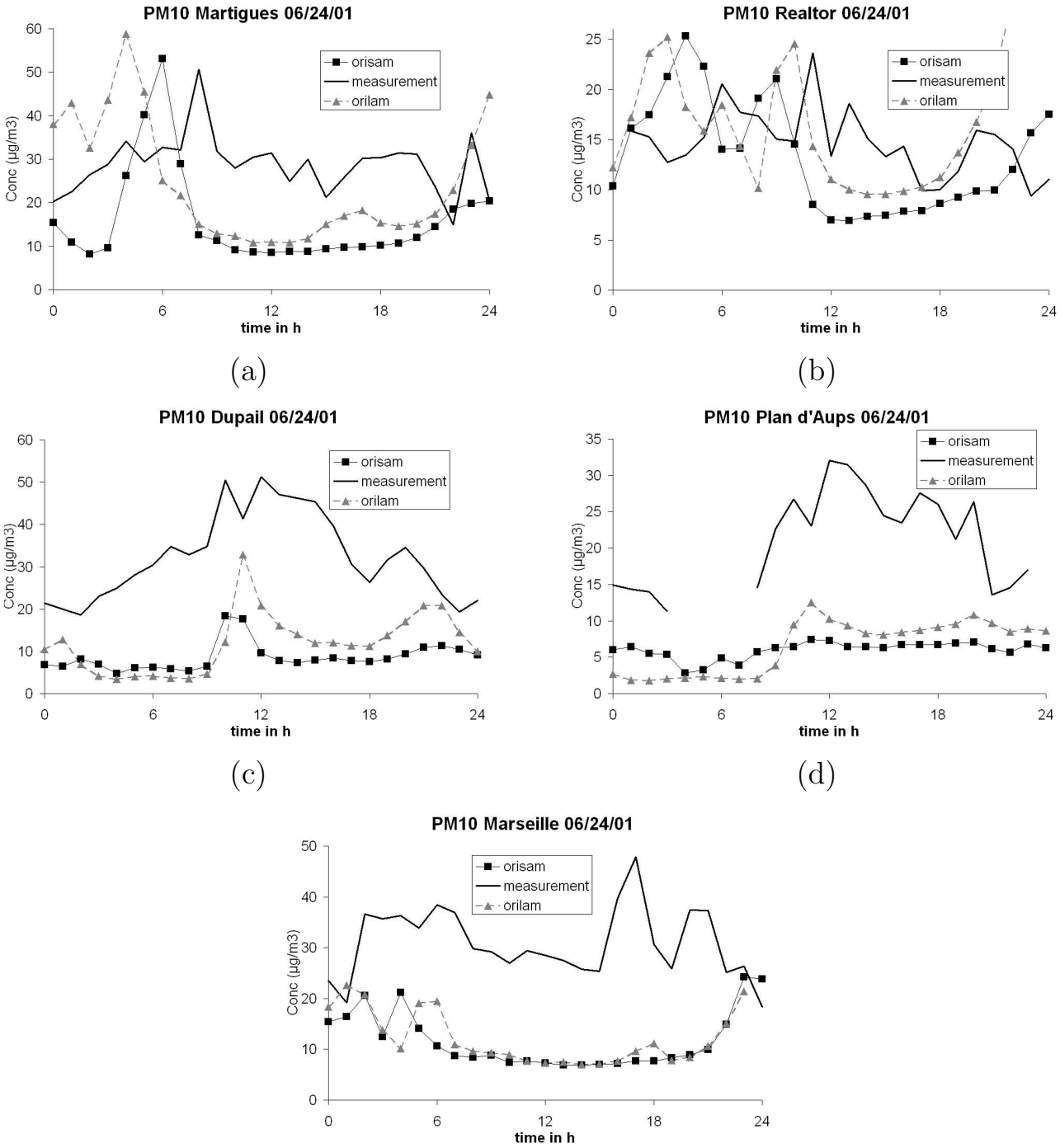

Figure 1:

Figure 3. PM-10 time series (scale in $\mu g.m^{-3}$ at the left) on June 24 at: (a) Martigues, (b) Realtor, (c) Dupail, (d) Plan d'Aups and (e) Marseille (dark curve for measurement, squares for ORISAM simulation in dark grey and grey triangle for ORILAM simulation).